

Exploiting NOMA/OMA for Multi-UAV Communications in Large-Scale Networks

Tianwei Hou, *Student Member, IEEE*, Yuanwei Liu, *Member, IEEE*,
Zhengyu Song, Xin Sun, Yue Chen, *Senior Member, IEEE*,

Abstract

This paper advocates a pair of strategies in non-orthogonal multiple access (NOMA) in unmanned aerial vehicles (UAVs) communications, where multiple UAVs play as new aerial communications platforms for serving terrestrial NOMA users. A new multiple UAVs framework with invoking stochastic geometry technique is proposed, in which a pair of practical strategies are considered: 1) UAV-Centric strategy for offloading actions and 2) User-Centric strategy for providing emergency communications. In order to provide practical insights for the proposed NOMA assisted UAV framework, an imperfect successive interference cancelation (ipSIC) scenario is taken into account. For both UAV-Centric strategy and User-Centric strategy, we derive new exact expressions for the coverage probability. We also derive new analytical results for orthogonal multiple access (OMA) for providing a benchmark scheme. The derived analytical results in both User-Centric strategy and UAV-Centric strategy explicitly indicate that the ipSIC coefficient is a dominant component in terms of coverage probability. Numerical results are provided to confirm that i) for both User-Centric strategy and UAV-Centric strategy, NOMA assisted multi-UAV networks is capable of outperforming OMA by setting power allocation factors and targeted rate properly; and ii) the coverage probability of NOMA assisted multi-UAV framework is affected to a large extent by ipSIC coefficient, target rates and power allocations factors of paired NOMA users.

Index Terms

Non-orthogonal multiple access, stochastic geometry, unmanned aerial vehicles.

This work is supported by the Fundamental Research Funds for the Central Universities under Grant XXXX. Part of this work was submitted to the IEEE International Conference on Communications, Shanghai, China, May 2019 [1]

T. Hou, Z. Song and X. Sun are with the School of Electronic and Information Engineering, Beijing Jiaotong University, Beijing 100044, China (email: 16111019@bjtu.edu.cn, xsun@bjtu.edu.cn, songzy@bjtu.edu.cn).

Y. Liu and Yue Chen are with School of Electronic Engineering and Computer Science, Queen Mary University of London, London E1 4NS, U.K. (e-mail: yuanwei.liu@qmul.ac.uk, yue.chen@qmul.ac.uk).

I. INTRODUCTION

In the past decades, much research effort has been directed towards developing remotely operated unmanned aerial vehicles (UAVs), which stand as a potential candidate of aerial base station (BS) to provide access services to wireless devices located on the ground [2] or in the sky [3]. UAV communications are also an effective approach to provide connectivity during temporary events and after disasters in the remote areas that lack cellular infrastructure [2]. As compared to conventional terrestrial communications, one distinct feature of UAV communication is that the existence of line-of-sight (LoS) is capable to offer stronger small-scale fading between UAV and the ground users due to the high altitude of UAVs, which brings both opportunities and challenges in the design of UAV cellular networks [3]. The distinctive channel characteristics for UAV networks were investigated in [4], where different types of small-scale fading channels, i.e., Loo model, Rayleigh model, Nakagami- m model, Rician model and Weibull model, were summarized to demonstrate the channel propagation of UAV networks. Generally speaking, Nakagami- m distribution and Rician distribution are used to approximate the fluctuations in the fading channel with LoS propagations. It is also worth noting that the fading parameter of Nakagami- m fading $m = \frac{(K+1)^2}{2K+1}$, the distribution of Nakagami- m is approximately Rician fading with parameter K [5, eq. (3.38)]. Due to the limited spectrum resources on board of a UAV, achieving higher spectrum efficiency is of paramount importance to reap maximum benefits from UAV based communication networks.

To exploit the spectrum efficiency in the next generation wireless networks and beyond, especially in the UAV communication networks, non-orthogonal multiple access (NOMA) is considered to be a promising technique [6], [7]. More specifically, in contrast to the conventional orthogonal multiple access (OMA) techniques, NOMA is capable of exploiting the available resources more efficiently by opportunistically capitalizing on the users specific channel conditions [8], and it is capable of serving multiple users at different quality-of-service (QoS) requirements in the same resource block [9]–[11]. To be more clear, NOMA technique sends the signal to multiple users simultaneously by power domain multiplexing within the same frequency, time and code block. The basic principles of NOMA techniques rely on the employment of superposition coding (SC) at the transmitter and successive interference cancelation (SIC) techniques at the receiver [6], [12], and hence multiple accessed users can be realized in the power domain via different power levels for users in the same resource block. Therefore, UAV networks can

serve multiple users simultaneously by utilizing NOMA techniques for enhancing the achievable spectrum efficiency.

A. Prior Work and Motivation

Regarding the literature of UAV networks, early research contributions have studied the performance of single UAV or multiple UAVs networks. The air-to-air channel characterization in [13], studied the influence of the altitude-dependent Rician K factor. This work indicated that the impact of the ground reflected multi-path fading reduces with increasing UAV altitude. It is also worth noting that Rayleigh fading channel [14], which is a well-known model in scattering environment, can be also used to model the UAV channel characteristics in the case of large elevation angles in the mixed-urban environment. Mozaffari *et al.* [3], [15] proposed a UAV network with LoS probability, which depends on the height of the UAV, the horizontal distance between the UAV and users, the carrier frequency and type of environment. For the case that LoS exists, a fixed LoS coefficient, e.g., an extra 20dB attenuation, is the dominant component of small-scale fading channels. Chetlur *et al.* [16] proposed a downlink UAV network, where UAVs are distributed in a finite 3-D network. A uniform binomial point process was invoked to model the proposed network. Zhang *et al.* [17] proposed two possible paradigms for UAV assisted cellular communications, namely, cellular-enabled UAV communication and UAV-assisted cellular communication. The trajectory of the UAV has optimized under connectivity-constrained. Liu *et al.* [18] proposed a multiple-input multiple-output (MIMO) assisted UAV network, where the UAV serves multiple users through multi-beam simultaneously. However, the prior research contributions [3], [13]–[18] mainly focus on addressing the effects of OMA assisted UAV networks. Therefore, new research on UAV under emerging next generation network architectures is needed.

Recently, the use of NOMA in wireless communication has attracted great interest. Ding *et al.* [19] evaluated the performance of NOMA with randomly deployed users, where order statistics and stochastic geometry tools were invoked to evaluate the performance of paired NOMA users. Some application scenarios of NOMA have been investigated in the previous literature. More particularly, Liu *et al.* [20] proposed an innovative model of cooperative NOMA with simultaneous wireless information and power transfer (SWIPT), where a NOMA cluster consists of two NOMA users, one that is located in a small disk and the other is in a ring with a larger external radius. Ding *et al.* [8] evaluated the performance of NOMA with fixed power

allocation (F-NOMA) and cognitive radio inspired NOMA (CR-NOMA), and the user pairing strategies were carefully discussed. The analytical results show that it is more preferable to pair users whose channel gains are more distinctive to improve the diversity order in F-NOMA, whereas CR-NOMA prefers to pair the users with the best channel conditions. Recently, an imperfect SIC scenario has attracted great interest. Due to the fact that SIC techniques are deployed at the receivers, the residues of the multiplexed signal detected by SIC technique cannot be ignored [21]. Once an error occurs for carrying out SIC at the user with better channel gain, the NOMA systems will suffer from the residual interference signal. Hence it is significant to examine the detrimental impacts of imperfect SIC for NOMA system. Hou *et al.* [22] evaluated the outage performance of NOMA downlink transmission in both LoS and NLoS scenarios. A potential future research direction for NOMA, called Rate-Splitting multiple access, has been proposed by Mao *et al.* [23]. The analytical results in [23] demonstrated that RSMA can outperform SDMA and NOMA in the multi-antenna system and comes with a lower complexity than NOMA. RSMA assisted multi-cell networks and multi-antenna assisted RSMA were also proposed in [24]. The results derived concluded that RSMA can provide rate, robustness and QoS enhancements over SDMA and NOMA. With the goal of enhancing the physical layer security of NOMA networks, Liu *et al.* [25] proposed a NOMA assisted physical layer security framework in large-scale networks, where both single antenna and multiple antenna aided transmission scenarios were considered.

Integrating UAVs and NOMA into cellular networks is considered to be a promising technique to significantly enhance the performance of terrestrial users in the next generation wireless system and beyond, where UAVs are deployed with single antenna or multi-antenna to serve ground users by OMA or NOMA [26], [27]. A general introduction of UAV communications has been proposed by Liu *et al.* [28]. Three case studies, i.e., performance evaluation, joint trajectory design, and machine learning assisted UAV deployment [29], were carried out in order to better understand NOMA enabled UAV networks. Some challenges were concluded for future research directions. Nguyen *et al.* [30] proposed a cooperative UAV network, where UAVs are used as a flying relay in wireless backhaul network. Hou *et al.* [27] proposed a MIMO-NOMA assisted UAV network, where the closed-form expressions of outage performance and ergodic rate were evaluated in the downlink scenario. A NOMA assisted uplink scenario of UAV communication was proposed by Mao *et al.* [31], where two special cases, i.e., egoistic and altruistic transmission strategies of the UAV, were considered to derive the optimized solutions. Han *et al.* [32] proposed

a UAV assisted millimeter-wave air-to-everything networks, where aerial access points provide access services to users located on the ground, air, and tower. The buildings were modeled as a Boolean line-segment process with the fixed height.

The previous contributions [26]–[28], [31], [32] mainly consider NOMA in single UAV cell, and thus do not account for inter-cell interferences. The research contributions in terms of conducting on multi-UAV aided NOMA networks are still in their infancy, particularly with the focus of potential association strategies. NOMA enhanced UAV networks design poses three additional challenges: i) NOMA technology brings additional intra-cell interference from the connected UAV to the served users; ii) UAV communication requires different fading channels to evaluate the channel gain of LoS/NLoS propagation. iii) the user association policy requires to be reconsidered in NOMA assisted UAV networks. In this article, aiming at tackling the aforementioned issues, by proposing two potential association strategies, namely UAV-Centric strategy and User-Centric strategy, for intelligently investigating the effect of NOMA assisted UAV network performance is desired. The motivation of proposing two strategies is that the User-Centric strategy is a promising solution for providing access services after disasters in the remote areas, where all of terrestrial users can be served by UAVs. On the contrary, the UAV-Centric strategy can be perfectly deployed in the dense networks, i.e., concerts or football matches, to provide supplementary access services for offloading actions. Stochastic geometry tools are invoked to provide the mathematical paradigm to model the spatial randomness of both UAVs and users in multi-UAV networks. In contrast to the conventional terrestrial communication structure, stochastic geometry is capable of analyzing the average performance of the mobility and flexibility of the UAV networks.

B. Contributions

In contract to most existing research contributions in context of UAV communications [27], [31], [32], which focus on single cell networks, we consider multi-cell set-up in this treatise. We propose two new NOMA assisted multi-UAV strategies, namely User-Centric strategy and UAV-Centric strategy. Based on the proposed strategies, the primary theoretical contributions can be summarized as follows:

- We develop two potential association strategies to address the impact of NOMA on the nearest user, namely User-Centric strategy and UAV-Centric strategy, where stochastic geometry approaches are invoked to model the locations of both UAVs and users.

- For the User-Centric strategy: we derive the exact analytical expressions of a typical user in the NOMA enhanced User-Centric strategy in terms of coverage probability. Additionally, we derive the exact expressions in terms of coverage probability for the OMA assisted User-Centric strategy. Our analytical results illustrate that the distance of previous round user has almost no effect on the coverage probability of the typical user.
- For the UAV-Centric strategy: we derive the exact analytical expressions of paired NOMA users in the NOMA enhanced UAV-Centric strategy in terms of coverage probability. The exact expressions in terms of coverage probability for the OMA case are derived. Our analytical results demonstrate that the coverage probability of the near user is zero in the case of poor SIC quality.
- Simulation results confirm our analysis, and illustrate that by setting power allocation factors and targeted rate properly, NOMA assisted multi-UAV frameworks has superior performance over OMA assisted multi-UAV frameworks in terms of coverage probability, which demonstrates the benefits of the proposed strategies. Our analytical results also illustrate that the coverage probability can be greatly enhanced by LoS links.

C. Organization

The rest of the paper is organized as follows. In Section II, the NOMA assisted User-Centric strategy is investigated for multi-UAV frameworks, where the UAV provides access services to all the users. In Section III, the NOMA assisted UAV-Centric strategy is investigated, where the UAV only provides access services to the restricted area. Our numerical results are demonstrated in Section IV for verifying our analysis, which is followed by the conclusion in Section V.

II. USER-CENTRIC STRATEGY FOR EMERGENCY COMMUNICATIONS

We first focus our attention on a scenario, where all the terrestrial users are needed to be served equally after disasters in the remote areas or in the rural areas. Motivated by this purpose, we propose User-Centric strategy for providing emergency access services to all the terrestrial users.

Focusing on downlink transmission scenarios, we consider the User-Centric strategy as shown in Fig. 1(a). In this article, the UAV equipped with a single antenna communicates with multiple users equipped with a single antenna each. The UAVs are distributed according to a HPPP Ψ with density λ . For the simplicity of theoretical analysis, as shown in Fig. 1(b), an user is located at the original point in the User-Centric strategy, which becomes the typical user. The

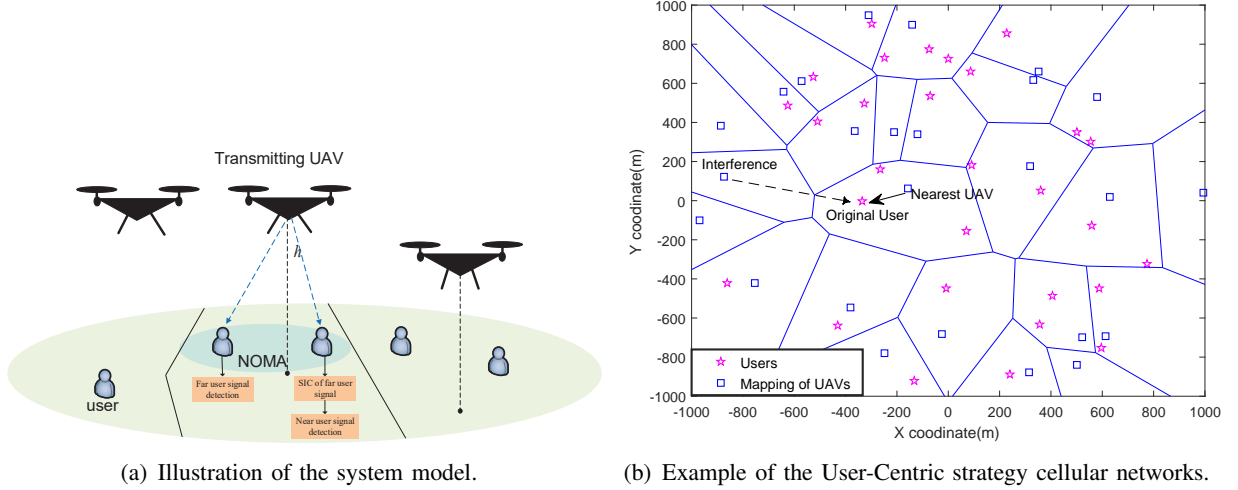


Fig. 1: Illustration of NOMA assisted User-Centric strategy model.

User-centric strategy is a useful model for the large-scale networks, i.e., field area, where users are uniformly located in the Voronoi cell according to a HPPP Φ_u with density λ_u . Unlike the UAV-Centric strategy, the User-Centric strategy considers that users are connected to the UAV one by one due to the fact that the number of users could be very small for the case of low user density. Without loss of generality, we consider that each UAV is associated with one user in the previous round of user association process. For simplicity, we assume that the horizontal distances between the associated users and the connected UAVs are the same, denoted by R_k , which can be any arbitrary values, and the horizontal distance between the typical user and the connected UAV is random, denoted by r .

A. Channel Model

Consider the use of a composite channel model with two parts, large-scale fading and small-scale fading. In the User-Centric strategy, for simplicity, we consider a two users case, where h_t and h_f denote the channel coefficients for the typical user and the fixed user, respectively. It is assumed that the horizontal distance r and the height of the UAV h are independent and identically distributed (i.i.d.). In this article, large-scale fading represents the path loss and shadowing between the UAV and users.

In order to better illustrate the LoS propagation between the UAV and user, the small-scale fading is defined by Nakagami- m fading as

$$f(x) = \frac{m^m x^{m-1}}{\Gamma(m)} e^{-mx}, \quad (1)$$

where m denotes the fading parameter, and $\Gamma(m)$ denotes Gamma function. Note that $\Gamma(m) = (m-1)!$ when m is an integer. In this paper, the UAV can be projected to the coverage disc by projection theorem. Thus, the distance between the UAV to the typical user can be written as

$$d_t = \sqrt{h^2 + r^2}. \quad (2)$$

In order to avoid infinite received power, it is assumed that the height of the UAV is greater than 1m to simplify the analytical results. Therefore, the large-scale fading can be expressed as

$$L_t = d_t^{-\alpha}, \quad (3)$$

where α denotes the path loss exponent. Thus, the received power from the associated UAV for the user at origin is given by

$$P_t = P_U L_t |h_t|^2, \quad (4)$$

where P_U denotes the transmit power of the UAV.

In downlink transmission, paired NOMA users also detect interference from neighboring UAVs. Therefore, the co-channel interference I can be further expressed as follows:

$$I \triangleq \sum_{j \in \Psi, d_j > d} |g_j|^2 P_U d_j^{-\alpha}, \quad (5)$$

where d_j and $|g_j|^2$ denote the distance and the small-scale fading between the user and the j -th interfering UAV.

Besides, it is assumed that the channel state information (CSI) of UAVs is perfectly known at the typical user. The signal-to-interference-plus-noise ratio (SINR) of the User-Centric strategy will be derived in the following subsection.

B. SINR Analysis

For the User-Centric strategy, since it is not pre-determined that the typical user is the near user or the far user, we have to provide all potential cases for the SINR analysis. Thus, on the one hand, for the far user case that the distance from the UAV to the typical user is larger than the fixed user, the typical user treats the signal from the fixed user as noise, and the SINR can be expressed as

$$SINR_{t, far} = \frac{|h_t|^2 d_t^{-\alpha} P_U \alpha_v^2}{\sigma^2 + |h_t|^2 d_t^{-\alpha} P_U \alpha_w^2 + \sum_{j \in \Psi} |g_j|^2 P_U d_{j,t}^{-\alpha}}, \quad (6)$$

where σ^2 denotes the additive white Gaussian noise (AWGN) power, α_v^2 and α_w^2 denote the power allocation factors for the far user and the near user, respectively. Note that $\alpha_v^2 + \alpha_w^2 = 1$ in NOMA communication.

Then, the fixed user needs to decode the information from the typical user with the SINR

$$SINR_{f \rightarrow t, near} = \frac{|h_f|^2 d_f^{-\alpha} P_U \alpha_v^2}{\sigma^2 + |h_f|^2 d_f^{-\alpha} P_U \alpha_w^2 + \sum_{j \in \Psi} |g_j|^2 P_U d_{j,f}^{-\alpha}}, \quad (7)$$

where d_f denotes the distance between the fixed user and the associated UAV with $d_f = \sqrt{R_k^2 + h^2}$.

Once it is decoded successfully, the fixed user will decode its own signal with imperfect SIC coefficient, and the SINR can be expressed as

$$SINR_{f, near} = \frac{|h_f|^2 d_f^{-\alpha} P_U \alpha_w^2}{\sigma^2 + \beta |h_f|^2 d_f^{-\alpha} P_U \alpha_v^2 + \sum_{j \in \Psi} |g_j|^2 P_U d_{j,f}^{-\alpha}}, \quad (8)$$

where β denotes the imperfect SIC coefficient. Since in practice that SIC is not perfect, a fraction $0 < \beta < 1$ is considered in our model for the user with better channel gain. On the one hand, $\beta = 0$ when perfect SIC is assumed, and the near user can be perfectly decode the signal intended for the far user. On the other hand, when SIC is failed or there is no corresponding SIC, $\beta = 1$.

On the other hand, when the typical user has smaller distance to the UAV than the fixed user, the SINR at the fixed user can be expressed as

$$SINR_{f, far} = \frac{|h_f|^2 d_f^{-\alpha} P_U \alpha_v^2}{\sigma^2 + |h_f|^2 d_f^{-\alpha} P_U \alpha_w^2 + \sum_{j \in \Psi} |g_j|^2 P_U d_{j,f}^{-\alpha}}. \quad (9)$$

Based on (7) and (8), The SINR at the typical user in the near user case can be expressed as

$$SINR_{t, near} = \frac{|h_t|^2 d_t^{-\alpha} P_U \alpha_w^2}{\sigma^2 + \beta |h_t|^2 d_t^{-\alpha} P_U \alpha_v^2 + \sum_{j \in \Psi} |g_j|^2 P_U d_{j,t}^{-\alpha}}, \quad (10)$$

if the typical user decodes the information from the fixed user successfully.

C. Coverage Probability of the User-Centric Strategy

In the networks considered, we first focus on analyzing the probability density functions (PDF) of user distance distributions for paired NOMA users, which will be used for both User-Centric

strategy and UAV-Centric strategy.

Lemma 1. *The UAVs are distributed according to a HPPP with density λ . It is assumed that an extra UAV or an extra user is located at the origin of the disc, which is under expectation over the HPPP. Thus, in this case, the distance D , which is the distance between the original UAV or the original user and other UAVs, follows the distribution*

$$f_D(x) = 2\pi\lambda x e^{-\pi\lambda x^2}, x \geq 0. \quad (11)$$

Then, we focus on analyzing the User-Centric strategy of the proposed framework in order to increase the system fairness. In the User-Centric strategy, the user association is based on connecting the nearest UAV at the users. As such, the first step is to derive the Laplace transform of interference for the typical user.

Lemma 2. *For the User-Centric strategy, the Laplace transform of interference distribution for the both NOMA users is given by*

$$\mathcal{L}_t(s) = \exp \left(-\frac{2\pi\lambda}{\alpha} \sum_{i=1}^{m_I} \binom{m_I}{i} \left(\frac{sP_U}{m_I} \right)^\delta (-1)^{\delta-i} B \left(\frac{-sP_U}{m_I r_t^\alpha}; i - \delta, 1 - m_I \right) \right), \quad (12)$$

where $r_t = \sqrt{x^2 + h^2}$, $\delta = \frac{2}{\alpha}$, x is the nearest horizontal distance allowed between a typical user and its connected UAV, and $B(\cdot)$ denotes incomplete Beta function.

Proof. Please refer to Appendix A. □

For the case of large-scale networks, the exist of LoS propagation between interfering UAVs at infinity and users is not reasonable. Thus, a special case that $\alpha = 4$ and $m_I = 1$ is worth estimating.

Corollary 1. *For the special case that the small scale fading channels between interference sources and users follow Rayleigh fading and $\alpha = 4$ of the User-Centric strategy, the Laplace transform of interference distribution for the both paired NOMA users can be transformed into*

$$\begin{aligned} \mathcal{L}_t(s) &\stackrel{(a)}{=} \exp \left(-\frac{2\pi\lambda P_U r_t^{2-\alpha}}{\alpha(1-\delta)} {}_2F_1(1, 1-\delta; 2-\delta; -sP_U r_t^{-\alpha}) \right) \\ &\stackrel{(b)}{=} \exp \left(-\pi\lambda \sqrt{sP_U} \tan^{-1} \left(\frac{\sqrt{sP_U}}{r_t^2} \right) \right), \end{aligned} \quad (13)$$

where (a) is resulted from applying $m_I = 1$, (b) is obtained by substituting $\alpha = 4$, and ${}_2F_1(; ;)$ denotes hypergeometric function.

Then, we focus on the coverage behavior of the User-Centric strategy. The fixed power allocation strategy is deployed at the UAV, where the power allocation factors α_w^2 and α_v^2 are constant during transmission. It is assumed that the target rates of the typical user and fixed user are R_t and R_f , respectively. Therefore, the coverage probability of the typical user is given in following two Lemmas.

Lemma 3. The conditional coverage probability of a typical user for the near user case in the User-Centric strategy is expressed in closed-form as

$$P_{cov,t,n}(x) = \sum_{n=0}^{m-1} \sum_{p=0}^n \binom{n}{p} \frac{(-1)^n}{n!} \Lambda_4^n \Lambda_5^n \exp \left(-m M_{t*} \sigma^2 r_t^\alpha - \Lambda_3 r_t^2 \right) r_t^{\alpha(1-j)q_j + (2-\alpha b)q_b + \alpha n}, \quad (14)$$

where $M_t^n = \frac{\varepsilon_t}{P_U(\alpha_w^2 - \beta \varepsilon_t \alpha_v^2)}$, $M_{t \rightarrow f} = \frac{\varepsilon_f}{P_U(\alpha_v^2 - \varepsilon_f \alpha_w^2)}$, $M_{t*} = \max \{M_t^n, M_{t \rightarrow f}\}$, $\varepsilon_t = 2^{R_t} - 1$, $\varepsilon_f = 2^{R_f} - 1$, $r_t = \sqrt{x^2 + h^2}$,

$$\Lambda_3 = \frac{2\pi m \lambda}{\alpha} \sum_{a=0}^{\infty} \frac{(m_I)_a}{a!(i-\delta+a)} \sum_{i=1}^{m_I} \binom{m_I}{i} \left(\frac{M_{t*} P_U}{m_I} \right)^{i+a} (-1)^a, \quad \Lambda_4^n = \sum p! \prod_{j=1}^p \frac{\left((-m M_{t*} \sigma^2) \prod_{k=0}^{j-1} (1-k) \right)^{q_j}}{q_j! (j!)^{q_j}}, \text{ and}$$

$$\Lambda_5^n = \sum (n-p)! \prod_{b=1}^{n-p} \frac{\left((-\Lambda_3) \prod_{k=0}^{b-1} (\delta-k) \right)^{q_b}}{q_b! (b!)^{q_b}}.$$

Proof. Please refer to Appendix B. □

Noth that decoding will succeed if the typical user can decode its own message by treating the signal from connected user as noise. The conditional coverage probability of a typical user for the far user case is calculated in the following Lemma.

Lemma 4. The conditional coverage probability of a typical user for the far user case in the User-Centric strategy is expressed in closed-form as

$$P_{cov,t,f}(x) = \sum_{n=0}^{m-1} \sum_{p=0}^n \binom{n}{p} \frac{(-1)^n}{n!} \Lambda_4^f \Lambda_5^f \exp \left(-m M_t^f \sigma^2 r_t^\alpha - \Lambda_3^f r_t^2 \right) r_t^{\alpha(1-j)q_j + (2-\alpha b)q_b + \alpha n}, \quad (15)$$

where $M_t^f = \frac{\varepsilon_t}{P_U(\alpha_v^2 - \varepsilon_t \alpha_w^2)}$, $\Lambda_3^f = \frac{2\pi m \lambda}{\alpha} \sum_{a=0}^{\infty} \frac{(m_I)_a}{a!(i-\delta+a)} \sum_{i=1}^{m_I} \binom{m_I}{i} \left(\frac{M_t^f P_U}{m_I} \right)^{i+a} (-1)^a$,

$$\Lambda_4^f = \sum p! \prod_{j=1}^p \frac{\left((-m M_t^f \sigma^2) \prod_{k=0}^{j-1} (1-k) \right)^{q_j}}{q_j! (j!)^{q_j}}, \text{ and } \Lambda_5^f = \sum (n-p)! \prod_{b=1}^{n-p} \frac{\left((-\Lambda_3^f) \prod_{k=0}^{b-1} (\delta-k) \right)^{q_b}}{q_b! (b!)^{q_b}}.$$

Proof. Based on the SINR analysis in (6), and following the similar procedure in Appendix B, with interchanging M_{t*} with M_t^f , we can obtain the desired result in (15). Thus, the proof is complete. \square

Based on **Lemma 3** and **Lemma 4**, the coverage probability of the typical user in the User-Centric strategy can be calculated in the following Theorem.

Theorem 1. The exact expression of the coverage probability for the typical user is expressed as

$$P_{cov,t} = \int_0^{R_k} P_{cov,t,n}(x) f(x) dx + \int_{R_k}^{\infty} P_{cov,t,f}(x) f(x) dx, \quad (16)$$

where $P_{cov,t,n}(x)$ is given in (14), $P_{cov,t,f}(x)$ is given in (15), and $f(x)$ is given in (11).

Proof. Considering the distance distributions of the typical user at the origin associated to the UAV with the serving distance R_k , which is distance of the associated user in previous round, we can readily obtain the desired results in (16). The proof is complete. \square

Remark 1. The derived results in (14) and (15) demonstrate that the coverage probability of a typical user is determined by the target rate of itself, fading parameter m of the small scale fading channels and the distance of the connected user served by the same UAV.

Remark 2. Inappropriate power allocation such as, $\alpha_v^2 - \varepsilon_t \alpha_w^2 < 0$ and $\alpha_w^2 - \beta \varepsilon_t \alpha_v^2 < 0$, will lead to the coverage probability always being zero.

In order to provide more insights of multi-UAV networks, the coverage probability of the typical user is also derived in the OMA case.

Corollary 2. The conditional coverage probability of a typical user for the OMA case in the User-Centric strategy is expressed in closed-form as

$$P_{cov,t,o}(x) = \sum_{n=0}^{m-1} \sum_{p=0}^n \binom{n}{p} \frac{(-1)^n}{n!} \Lambda_4^o \Lambda_5^o \exp(-m M_t^o \sigma^2 r_t^\alpha - \Lambda_3^o r_t^2) r_t^{\alpha(1-j)q_j + (2-\alpha b)q_b + \alpha n}, \quad (17)$$

where $M_t^o = \frac{\varepsilon_t^o}{P_U}$, $\varepsilon_t^o = 2^{2R_t} - 1$, $\Lambda_3^o = \frac{2\pi m \lambda}{\alpha} \sum_{a=0}^{\infty} \frac{(m_I)_a}{a!(i-\delta+a)} \sum_{i=1}^{m_I} \binom{m_I}{i} \left(\frac{M_t^o P_U}{m_I}\right)^{i+a} (-1)^a$,

$$\Lambda_4^o = \sum p! \prod_{j=1}^p \frac{\left((-m M_t^o \sigma^2) \prod_{k=0}^{j-1} (1-k)\right)^{q_j}}{q_j! (j!)^{q_j}}, \text{ and } \Lambda_5^o = \sum (n-p)! \prod_{b=1}^{n-p} \frac{\left((- \Lambda_3) \prod_{k=0}^{b-1} (\delta-k)\right)^{q_b}}{q_b! (b!)^{q_b}}.$$

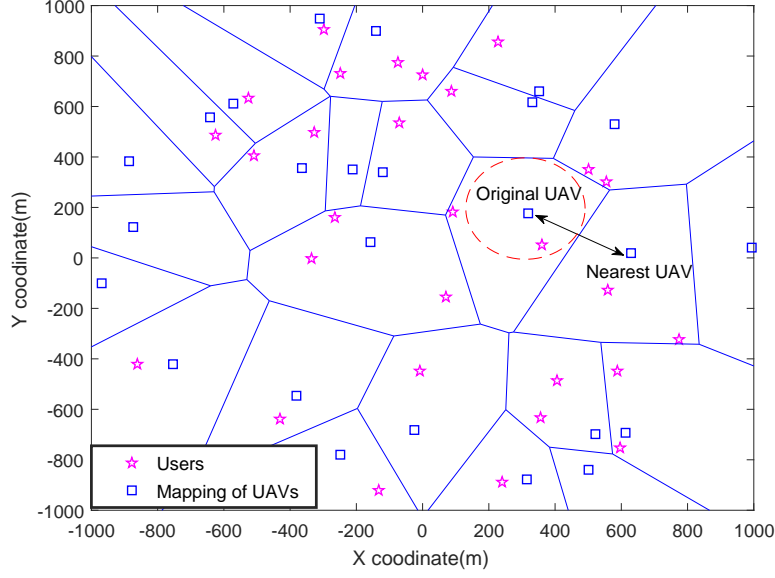


Fig. 2: Example of the UAV-Centric strategy cellular networks.

Proof. Following the similar procedure in Appendix B, with interchanging M_t^f with M_t^o , we can obtain the desired result in (17). Thus, the proof is complete. \square

III. UAV-CENTRIC STRATEGY FOR OFFLOADING ACTIONS

In conventional BS communication system, the BS are distributed in order to cover all the ground, whereas UAV communications mainly focus on providing access services to support BS in the dense networks, i.e., airports or resorts, where most people are located in the lounge. Motivated by this purpose, and on the basis of the above User-Centric strategy, another strategy considered in this paper is the UAV-Centric strategy, where paired NOMA users are located inside the coverage disc as shown in Fig. 2.

For the UAV-Centric strategy, an UAV is located at the original point, which becomes the typical UAV serving users in the typical cell. Therefore, it is assumed that the distance between the UAV at the origin and the nearest UAV is D , and the potential paired NOMA users are located in the coverage area within the radius $D/2$. In the UAV-Centric strategy, user pairing strategy is determined by the connected UAV, where all the users in the coverage disc are connected to the UAV. For simplicity, two users, near user w and far user v , access to the UAV at the origin. It is assumed that the users are uniformly located, which is according to HPPP, denoted by Ψ_u and it is associated with the density λ_u , within large ring and small disc with radius $D/2$ and $D/4$, respectively. In the UAV-Centric strategy, h_w and h_v denote the channel coefficients for the near user and the far user, respectively.

A. SINR Analysis

For the UAV-Centric strategy, the distances between the interfering UAVs and the users are more complicated. For notational simplicity, the location of the j -th interfering UAV is denoted by y_j , where $y_j \in \Psi$. The locations of the cluster users are conditioned on the locations of their cluster heads (UAVs). As such, the distance from a user to its UAV is simply given by $\|x_i\|$, where $\|x_i\|$ denotes the Euclidean distance of the user i . In this article, we only focus on the users in the typical cell, and the distance between the user and interfering UAV j is denoted by $d_j = \left\| \sqrt{(y_j - x_i)^2 + h^2} \right\|$. Thus, the SINR of the far user v can be derived as

$$SINR_v = \frac{|h_v|^2 d_v^{-\alpha} P_U \alpha_v^2}{\sigma^2 + |h_v|^2 d_v^{-\alpha} P_U \alpha_w^2 + \sum_{j \in \Psi} |g_{j,v}|^2 P_U d_{j,v}^{-\alpha}}, \quad (18)$$

where $|g_{j,v}|^2$ and $d_{j,v}$ denote the small scale fading channels and the distance between j -th interfering UAV and the far user, respectively.

The near user w will first decode the signal of the far user v with the following SINR

$$SINR_{w \rightarrow v} = \frac{|h_w|^2 d_w^{-\alpha} P_U \alpha_v^2}{\sigma^2 + \beta |h_w|^2 d_w^{-\alpha} P_U \alpha_w^2 + \sum_{j \in \Psi} |g_{j,w}|^2 P_U d_{j,w}^{-\alpha}}. \quad (19)$$

If the signal of the v -th user can be decoded successfully, the w -th user then decodes its own signal. As such, the SINR at the w -th user can be expressed as

$$SINR_w = \frac{|h_w|^2 d_w^{-\alpha} P_U \alpha_w^2}{\sigma^2 + \beta |h_w|^2 d_w^{-\alpha} P_U \alpha_v^2 + \sum_{j \in \Psi} |g_{j,w}|^2 P_U d_{j,w}^{-\alpha}}. \quad (20)$$

B. Coverage Probability of the UAV-Centric Strategy

Consider a disk centered at the origin with the radius $D/2$, which has shown in Fig. 2. In order to deploy NOMA protocol, we separate the disc to two parts equally, the small disc with radius $D/4$ and the ring with radius from $D/4$ to $D/2$, to serve paired NOMA users. It is assumed that the near users and the far users are located in the small disc and ring, respectively. Focusing on the typical cell, which located at the origin, the link distance between a user uniformly distributed in the small disc, and conditioned on D , follows

$$f_{R|D}(r|D) = \frac{32r}{D^2}, 0 \leq r \leq l_1, \quad (21)$$

where $l_1 = \frac{D}{4}$.

The PDF of far users can be obtained by

$$f_{R|D}(r|D) = \frac{32r}{3D^2}, l_1 \leq r \leq l_2, \quad (22)$$

where $l_2 = \frac{D}{2}$.

In order to derive the system performance, the Laplace transform of interfering UAVs needs to be derived. We calculate the Laplace transform of inter-cell interference for the paired users in the following Lemma.

Lemma 5. *For the UAV-Centric strategy, the Laplace transform of interference distribution conditioned on the serving distance D for the near user is given by*

$$\begin{aligned} \mathcal{L}_U(s|D) = & \exp\left(-\frac{l_I}{D} \left(1 - \left(1 + \frac{SP_u}{m_I l_I^\alpha}\right)^{-m_I}\right)\right) \\ & \times \exp\left(-\frac{2\pi\lambda_U}{\alpha} \sum_{i=1}^{m_I} \binom{m_I}{i} \left(\frac{sP_U}{m_I}\right)^\delta (-1)^{(\delta-i)} B\left(\frac{-sP_U l_I^{-\alpha}}{m_I}; i - \delta, 1 - m_I\right)\right). \end{aligned} \quad (23)$$

where $l_I = \sqrt{D^2 + h^2}$.

Proof. Please refer to Appendix C. □

It's also worth noting that for the case of low UAV density, the small-scale fading between users and interfering UAVs can be considered to Rayleigh fading. Thus, the Laplace transform can be further obtained in the following Corollary.

Corollary 3. *For the near user in the case of low UAV density, the Laplace transform of interference distribution conditioned on the serving distance D is given by*

$$\mathcal{L}_U(s|D) = \exp\left(-\frac{l_I}{D} \left(\frac{SP_u}{l_I^\alpha + SP_u}\right)\right) \exp\left(-\frac{2\pi\lambda_U P_U l_I^{2-\alpha}}{\alpha(1-\delta)} {}_2F_1(1, 1-\delta; 2-\delta; -sP_U l_I^{-\alpha})\right). \quad (24)$$

Then, we focus on the coverage behavior of the near user w , who is the user with higher channel gain. In the UAV-Centric strategy, the coverage probability is more complicated than the User-Centric strategy due to the fact that an extra interference source, the first interference, is necessary to evaluate separately. It is assumed that the target rates of user w and user v are R_w and R_v , respectively. Therefore, the coverage probability of the w -th user is given in the following Lemma.

Lemma 6. The closed-form expression of the conditional coverage probability on serving distance for the near user is expressed as

$$P_{cov,w}(r|D) = \sum_{n=0}^{m-1} \sum_{k=0}^n \sum_{l=0}^k \frac{(-1)^n r_w^{\alpha n}}{l!(k-l)!(n-k)!} \Theta_3 \Theta_4 \Theta_5 \quad (25)$$

$$\times \exp \left(-m M_{w*} \sigma^2 r_w^\alpha - \Theta_1 r_w^{\alpha(i+a)} - \frac{m l_I}{D} + \Theta_2 r_w^{\alpha u} \right) r_w^{\alpha(1-j)q_j + \alpha(i+a-g)q_g + \alpha n + \alpha(u-b)q_u},$$

where $M_w = \frac{\varepsilon_w}{P_U(\alpha_w^2 - \beta \varepsilon_w \alpha_v^2)}$, $M_v = \frac{\varepsilon_v}{P_U(\alpha_v^2 - \varepsilon_v \alpha_w^2)}$, $\varepsilon_w = 2^{R_w} - 1$, $\varepsilon_v = 2^{R_v} - 1$, $M_{w*} = \max\{M_w, M_v\}$, $r_w = \sqrt{r^2 + h^2}$, $\Theta_1 = \pi m \delta \lambda \sum_{i=1}^{m_I} \binom{m_I}{i} (-1)^{\delta-1} \sum_{a=0}^{\infty} \frac{(m_I)_a}{a!(i-\delta+a)} \left(\frac{M_{w*} P_U}{m_I} \right)^{i+a} l_I^{-\alpha(i-\delta+a)}$,

$$\Theta_2 = \frac{m l_I}{D} \sum_{u=0}^{\infty} (-1)^u C_{m_I+u+1}^u \left(\frac{M_{w*} P_U}{l_I^{\alpha} m_I} \right)^u, \quad \Theta_3 = \sum (n-k)! \prod_{j=1}^{n-k} \frac{\left((-m M_{w*} \sigma^2) \prod_{p=0}^{j-1} (1-p) \right)^{q_j}}{q_j! (j!)^{q_j}},$$

$$\Theta_4 = \sum (k-l)! \prod_{b=1}^{k-l} \frac{\left((-\Theta_2) \prod_{p=0}^{b-1} (u-p) \right)^{q_u}}{q_u! (j!)^{q_u}}, \quad \text{and } \Theta_5 = \sum l! \prod_{g=1}^l \frac{\left((-\Theta_1) \prod_{p=0}^{g-1} (i+a-g) \right)^{q_g}}{q_g! (j!)^{q_g}}.$$

Proof. Please refer to Appendix D. \square

Similar to **Lemma 6**, the coverage probability of the far user can be derived in the following Lemma.

Lemma 7. The closed-form expression of the conditional coverage probability on serving distance for the far user is expressed as

$$P_{cov,v}(r|D) = \sum_{n=0}^{m-1} \sum_{k=0}^n \sum_{l=0}^k \frac{(-1)^n r_v^{\alpha n}}{l!(k-l)!(n-k)!} \Theta_{3,v} \Theta_{4,v} \Theta_{5,v} \quad (26)$$

$$\times \exp \left(-m M_v \sigma^2 r_v^\alpha - \Theta_{1,v} r_v^{\alpha(i+a)} - \frac{m l_I}{D} + \Theta_{2,v} r_v^{\alpha u} \right) r_v^{\alpha(1-j)q_j + \alpha(i+a-g)q_g + \alpha n + \alpha(u-b)q_u},$$

where $r_v = \sqrt{r^2 + h^2}$, $\Theta_{1,v} = \pi m \delta \lambda \sum_{i=1}^{m_I} \binom{m_I}{i} (-1)^{\delta-1} \sum_{a=0}^{\infty} \frac{(m_I)_a}{a!(i-\delta+a)} \left(\frac{M_v P_U}{m_I} \right)^{i+a} l_I^{-\alpha(i-\delta+a)}$,

$$\Theta_{2,v} = \frac{m l_I}{D} \sum_{u=0}^{\infty} (-1)^u C_{m_I+u+1}^u \left(\frac{M_v P_U}{l_I^{\alpha} m_I} \right)^u, \quad \Theta_{3,v} = \sum (n-k)! \prod_{j=1}^{n-k} \frac{\left((-m M_v \sigma^2) \prod_{p=0}^{j-1} (1-p) \right)^{q_j}}{q_j! (j!)^{q_j}},$$

$$\Theta_{4,v} = \sum (k-l)! \prod_{b=1}^{k-l} \frac{\left((-\Theta_{2,v}) \prod_{p=0}^{b-1} (u-p) \right)^{q_u}}{q_u! (j!)^{q_u}}, \quad \text{and } \Theta_{5,v} = \sum l! \prod_{g=1}^l \frac{\left((-\Theta_{1,v}) \prod_{p=0}^{g-1} (i+a-g) \right)^{q_g}}{q_g! (j!)^{q_g}}.$$

Proof. Similar to Appendix D, the derivation in (26) can be readily proved. \square

Then, the coverage probability of the paired NOMA user in the UAV-Centric strategy can be derived in the following Theorem.

Theorem 2. Based on **Lemma 6**, the exact expressions of the coverage probability for the paired NOMA users can be expressed as

$$P_{cov,w} = \int_0^\infty \int_0^{l_1} P_{cov,w}(r) f_{R|D}(r|D) dr f_D(D) dD, \quad (27)$$

and

$$P_{cov,v} = \int_0^\infty \int_{l_1}^{l_2} P_{cov,v}(r) f_{R|D}(r|D) dr f_D(D) dD, \quad (28)$$

where $l_1 = \frac{D}{4}$, $l_2 = \frac{D}{2}$, $P_{cov,w}(r)$ is given in (25), $P_{cov,v}(r)$ is given in (26), $f_{R|D}(r|D)$ is given in (21), and $f_D(D)$ is given in (11).

Proof. Please refer to Appendix E. □

In order to provide more engineering insights, the coverage probability for the near user in the OMA assisted UAV-Centric strategy is also derived in the following Corollary.

Corollary 4. The conditional coverage probability of the near user for the OMA case in the UAV-Centric strategy is expressed in closed-form as

$$P_{cov,w}^o(r|D) = \sum_{n=0}^{m-1} \sum_{k=0}^n \sum_{l=0}^k \frac{(-1)^n r_w^{\alpha n}}{l!(k-l)!(n-k)!} \Theta_3^o \Theta_4^o \Theta_5^o \times \exp \left(-m M_w^o \sigma^2 r_w^\alpha - \Theta_1 r_w^{\alpha(i+a)} - \frac{m l_I}{D} + \Theta_2 r_w^{\alpha u} \right) r_w^{\alpha(1-j)q_j + \alpha(i+a-g)q_g + \alpha n + \alpha(u-b)q_u}, \quad (29)$$

where $M_w^o = \frac{\varepsilon_w^o}{P_U}$, $\varepsilon_w^o = 2^{2R_w} - 1$, $\Theta_1^o = \pi m \delta \lambda \sum_{i=1}^{m_I} \binom{m_I}{i} (-1)^{\delta-1} \sum_{a=0}^{\infty} \frac{(m_I)_a}{a!(i-\delta+a)} \left(\frac{M_w^o P_U}{m_I} \right)^{i+a} l_I^{-\alpha(i-\delta+a)}$,
 $\Theta_2^o = \frac{m l_I}{D} \sum_{u=0}^{\infty} (-1)^u C_{m_I+u+1}^u \left(\frac{M_w^o P_U}{l_I^\alpha m_I} \right)^u$, $\Theta_3^o = \sum (n-k)! \prod_{j=1}^{n-k} \frac{\left((-m M_w^o \sigma^2) \prod_{p=0}^{j-1} (1-p) \right)^{q_j}}{q_j! (j!)^{q_j}}$,
 $\Theta_4^o = \sum (k-l)! \prod_{b=1}^{k-l} \frac{\left((-\Theta_2^o) \prod_{p=0}^{b-1} (u-p) \right)^{q_u}}{q_u! (j!)^{q_u}}$, and $\Theta_5^o = \sum l! \prod_{g=1}^l \frac{\left((-\Theta_1^o) \prod_{p=0}^{g-1} (i+a-g) \right)^{q_g}}{q_g! (j!)^{q_g}} ..$

Proof. Following the similar procedure in Appendix D, with interchanging M_w^f with M_w^o , we can obtain the desired result in (29). Thus, the proof is complete. □

IV. NUMERICAL STUDIES

In this section, numerical results are provided to facilitate the performance evaluation of NOMA assisted multi-UAV networks. Monte Carlo simulations are conducted to verify analytical

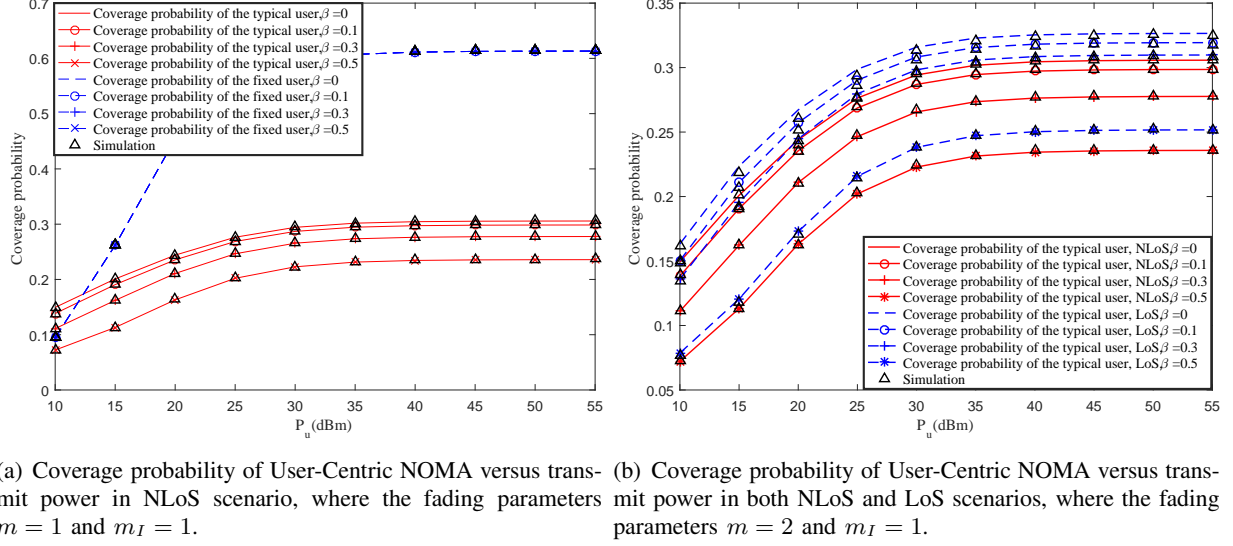


Fig. 3: Coverage probability of paired NOMA users versus the power of UAV in the User-Centric strategy, with target rate $R_t = 1$ bits per channel use (BPCU) and $R_f = 0.5$ BPCU. The height of the UAV is fixed to 50m, and the horizontal distance of the fixed user is 300m. The exact results of NOMA are calculated from (16).

results. In the considered network, it is assumed that the power allocation factors are $\alpha_v^2 = 0.6$ for the far user and $\alpha_w^2 = 0.4$ for the near user. The path loss exponent $\alpha = 4$. In Monte Carlo simulations, it is not possible to simulate a real infinite distribution for UAVs. Hence, the UAVs are distributed in a disc, and the radius of the disc is $10000m$. The power of AWGN noise is set as $\sigma^2 = -90$ dBm. The UAV density $\lambda = \frac{1}{500^2\pi}$. It is also worth noting that LoS and NLoS scenarios are indicated by the Nakagami fading parameter m , where $m = 1$ for NLoS scenarios (Rayleigh fading) and $m > 1$ for LoS scenarios. Without loss of generality, we use $m = 2$ to represents LoS scenario in Section IV.

A. User-Centric Strategy

First, we evaluate the coverage performance of downlink NOMA users in the User-Centric strategy. In Fig. 3(a), for a given set of the distance of fixed users, the solid curves and dashed curves are the coverage probability for typical users and fixed users, respectively. We can see that, as the power of UAV increases, the coverage ceilings of both typical users and fixed NOMA users occur. This is due to the fact that, as the higher power level of interfering UAVs is deployed, the received SINR decreases dramatically. It is observed that as imperfect SIC coefficient β increases, the coverage probability of typical users decreases, which indicates that the performance of NOMA assisted UAV communication can be effectively improved by decreasing the imperfect

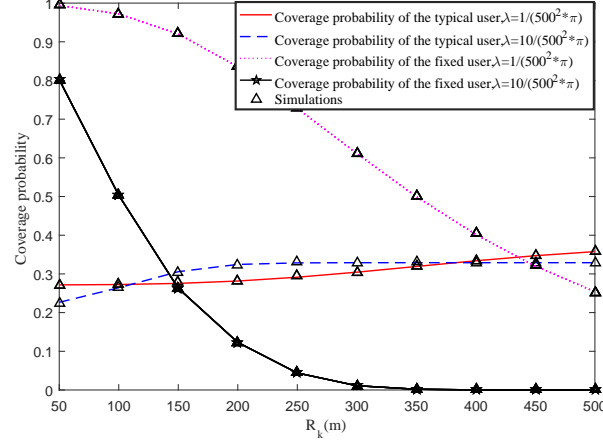


Fig. 4: Coverage probability of User-Centric NOMA versus the distance of fixed users, with target rate $R_t = 1$ BPCU and $R_f = 0.5$ BPCU. The height of the UAV is fixed to 50m, and the power of UAV is fixed to 40dBm.

SIC coefficient. For example, for the case of $\beta = \frac{2}{3}$, the power residual from imperfect SIC is greater than the power of near users, i.e., $\alpha_w^2 < \alpha_v^2\beta$. We can also see that for the case of $\beta = 0, 0.1, 0.3, 0.5$, the coverage probabilities of fixed users are the same. This is due to the fact that the imperfect SIC is the critical component of typical users, whereas the imperfect SIC has no effect for fixed users for the case $R_f = 0.5$ BPCU. As we can see in the figure, the outage of typical users occurs more frequently than fixed users. This is due to the fact that the chosen of power allocation factors and the distance of the fixed user. Note that the simulation results and analytical results match perfectly in Fig. 3(a), which demonstrate the accuracy of the developed analytical results.

Fig. 3(b) shows the coverage probability achieved by typical users in both NLoS and LoS scenario. In order to better illustrate the performance affected by the LoS transmission, the NLoS case is also shown in the figure as a benchmark for comparison. In Fig. 3(b), we can see that higher fading parameter m would result in reduced outage probability for different UAV power levels and different imperfect SIC coefficients. This is because that the LoS link between the UAV and users provides higher received power level. It is also worth noting that for the multi-UAV networks, the proposed network is not in need of a larger UAV power for increasing the coverage probability due to the fact that the error floor occurs in the high SNR regime.

In Fig. 4, the impact of different choices of UAV density and the distance of fixed users is studied. As can be observed from the figure, increasing the distance of fixed users will decrease the coverage probability for fixed users, whereas the coverage probability of typical users changes

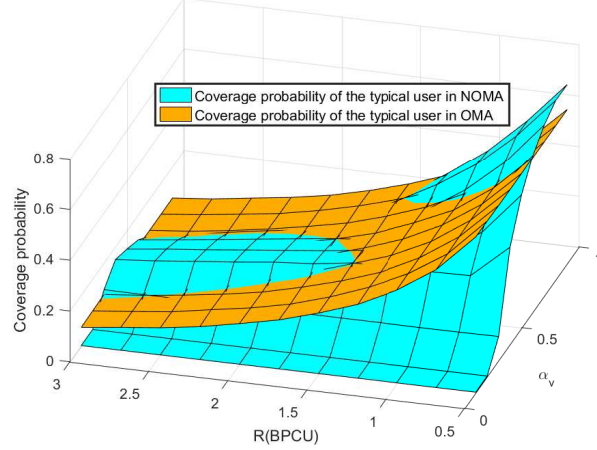


Fig. 5: Coverage probability of typical users versus targeted rate $R_t = R$ BPCU, and power allocation factor α_v , with the imperfect SIC coefficient $\beta = 0.05$. The target rate of fixed users $R_f = 0.5$ BPCU, The height of the UAV is fixed to 50m, and the horizontal distance of the fixed user is 300m. The transmit power of UAVs is fixed to 40dBm. The fading parameters $m = 3$ and $m_I = 2$.

slightly. This is due to the fact that the location distribution of typical users is not affected by fixed users. For fixed users, the received power decreases dramatically when the distance increases. On the other hand, for the dashed curve and star curves, where the density of UAV is 10 times greater than the solid curve and dotted curves, the coverage probability of fixed NOMA users is much smaller. This is because that the number of interfering UAVs is increased, which leads to the increase of received interference power level for both paired NOMA users. It is also worth noting that there are two crosses of typical users, which mean that there exists an optimal distance of fixed users for the given UAV density.

Next, Fig. 5 plots the coverage probability of typical users versus target rate R and power allocation factor α_v . It is observed that the coverage probability is zero in the case of inappropriate target rates and power allocation factors, which verifies the insights from **Remark 2**. The coverage probability of typical users in OMA is also plotted, which indicates that NOMA is capable for outperforming OMA for the appropriate power allocation factors and target rates of paired users even in the case of $\beta = 0.05$.

B. UAV-Centric strategy

In the UAV-Centric strategy, $\varepsilon = 0.1m$ to evaluate the interference received from the UAV located at the distance D . Then, we evaluate the performance of the downlink users in the UAV-Centric strategy. In Figs. 6(a) and 6(b), the impact of the NOMA assisted UAV-Centric

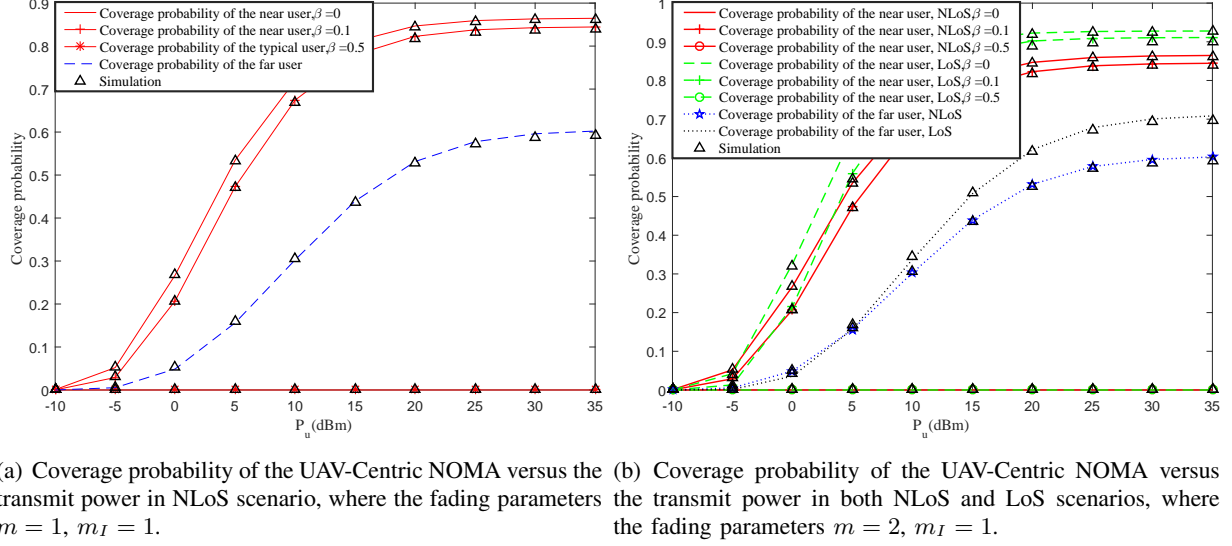


Fig. 6: Coverage probability of paired NOMA users versus the transmit power, with target rate $R_w = 1.5$ and $R_v = 1$ BPCU, respectively. The height of the UAV is fixed to 100m. The exact results of NOMA are calculated from (27).

strategy on the coverage probability is studied. The target rates of near users and far users are set as $R_w = 1.5$ BPCU and $R_v = 1$ BPCU, respectively. Solid curves and dashed curve are the coverage probability of near users and far users, respectively. An interesting phenomenon occurs in the UAV-Centric strategy that for the case $\beta = 0.5$, the coverage probability of near users is all zero, which indicates that the transmission is failed. This is again due to the fact that $\alpha_w^2 - \beta\alpha_v^2\varepsilon_w < 0$, which verifies our obtained insights in **Remark 2**.

Comparing Fig. 6(a) with Fig. 6(b), one can observe that the impact of fading parameter m on the coverage probability is also significant, which is due to the fact that the received power level is greater in the case of larger m . Again, we can see that the coverage probability is also one of near users in the case of $\beta = 0.5$, which indicates that the LoS propagation has no effect on **Remark 2**.

Fig. 7 plots the coverage probability for near users in the UAV-Centric strategy in the cases of $\beta = 0$, $\beta = 0.1$, and $\beta = 0.5$. One can obtain that on the one hand, inappropriate power allocation will lead to the coverage probability always being zero, which also verified **Remark 2**. On the other hand, we can see that for the case of $\beta > 0$, the coverage probability decreases dramatically when increasing target rate, which verified that the SIC residue is the dominant interference in NOMA. In order to provide more insights, the coverage performance of OMA in the UAV-Centric strategy is also provided. We can see that for the case of $\beta = 0$, NOMA

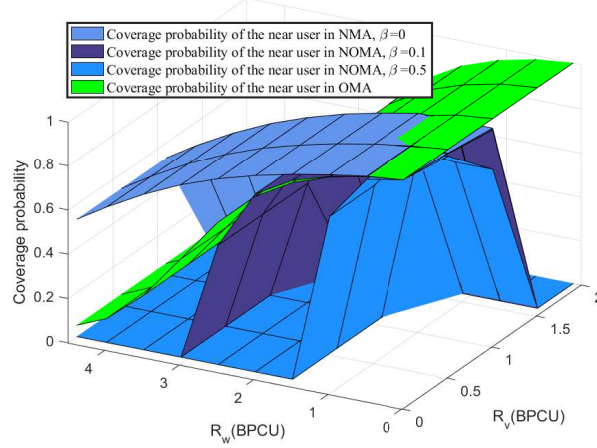


Fig. 7: Coverage probability of the near user versus the target rate, with the fixed serving height $h = 100\text{m}$. The transmit power of UAVs is fixed to 40dBm . The fading parameters $m = 3$ and $m_I = 2$.

performs better than OMA, which indicates that the proposed frameworks are analytically shown to be applicable for UAV communications.

V. CONCLUSIONS

In this article, we first proposed an overview on a pair of important new paradigms in multi-UAV communications, namely, User-Centric strategy and UAV-Centric strategy. The User-Centric strategy is applicable for the case when all the users located in the Voronoi cell are needed to be served by the UAV simultaneously. The derived results provide the benchmark for the NOMA assisted UAV cellular networks. The UAV-Centric strategy is motivated by the fact that, in practice, it is more applicable to serve users in the dense networks. The key idea of the UAV-Centric strategy is to provide services for the hotspots area only, i.e., airports or resorts. Then, the performance of proposed framework were evaluated, where multi-UAV are distributed in the sky to serve multiple users on the terrestrial. Additionally, new analytical expressions for interference and coverage probability were derived for characterizing the performance in NOMA assisted multi-UAV frameworks. An important future direction is to extend the 3-D distribution of interference sources to include other interfering UAVs located on the different height.

APPENDIX A: PROOF OF LEMMA 2

Consider a HPPP Ψ with density λ , the Laplace transform of the interference for the typical user can be expressed as follows:

$$\mathcal{L}_t(s) = \mathbb{E} \{ \exp(-sI_{t,\Psi}) \} = \mathbb{E} \left\{ \exp \left(-s \sum_{j \in \Psi, d_j > r_t} |g_j|^2 \frac{P_U}{m_I} d_j^{-\alpha} \right) \right\}, \quad (\text{A.1})$$

where $r_t = \sqrt{x^2 + h^2}$, x is the nearest horizontal distance allowed between a typical user and its connected UAV.

Using the moment generating function (MGF) of Gamma random variable $|g_j|$, the Laplace transform can be rewritten to

$$\mathcal{L}_t(s) = \exp \left(-2\pi\lambda \int_{r_t}^{\infty} \left(1 - \mathbb{E}_g \left\{ \exp \left(-s|g_j|^2 \frac{P_U}{m_I} r^{-\alpha} \right) \right\} \right) r dr \right). \quad (\text{A.2})$$

With the aid of Laplace transform for the Nakagami- m distribution with fading parameter m_I , we can obtain $\mathbb{E}_g \left\{ s|g_j|^2 \frac{P_U}{m_I} d^{-\alpha} \right\} = \left(1 + \frac{sP_U r^{-\alpha}}{m_I} \right)^{-m_I}$. As such, by applying binomial expansion, the Laplace transform of the typical user can be rewritten to

$$\begin{aligned} \mathcal{L}_t(s) &= \exp \left(-2\pi\lambda \int_{r_t}^{\infty} \left(1 - \left(1 + \frac{sP_U r^{-\alpha}}{m_I} \right)^{-m_I} \right) r dr \right) \\ &= \exp \left(-2\pi\lambda \int_{r_t}^{\infty} \frac{\sum_{i=0}^{m_I} \binom{m_I}{i} \left(\frac{sP_U}{r^\alpha m_I} \right)^i - 1}{\left(1 + \frac{sP_U r^{-\alpha}}{m_I} \right)^{m_I}} r dr \right). \end{aligned} \quad (\text{A.3})$$

Then, after some algebraic manipulations, we have

$$\begin{aligned} \mathcal{L}_t(s) &= \exp \left(-2\pi\lambda \sum_{i=1}^{m_I} \binom{m_I}{i} \left(\frac{sP_U}{m_I} \right)^i \int_{r_t}^{\infty} \frac{r^{-\alpha i + 1}}{\left(1 + \frac{sP_U r^{-\alpha}}{m_I} \right)^{m_I}} dr \right) \\ &\stackrel{(a)}{=} \exp \left(-\frac{2\pi\lambda}{\alpha} \sum_{i=1}^{m_I} \binom{m_I}{i} \left(\frac{sP_U}{m_I} \right)^\delta (-1)^{\delta-1} \int_0^{-\frac{sP_U}{r_t^\alpha m_I}} \frac{t^{i-\delta-1}}{(1-t)^{m_I}} dt \right), \end{aligned} \quad (\text{A.4})$$

where (a) is obtained by using $t = -\frac{sP_U}{r^\alpha m_I}$. Based on [33, eq. (8.391)], we can finally obtain

the Laplace transform of the typical user in the User-Centric strategy as follows:

$$\mathcal{L}_t(s) = \exp \left(-\frac{2\pi\lambda}{\alpha} \sum_{i=1}^{m_I} \binom{m_I}{i} \left(\frac{sP_U}{m_I} \right)^\delta (-1)^{(\delta-i)} B \left(\frac{-sP_U}{r_t^\alpha m_I}; i - \delta, 1 - m_I \right) \right). \quad (\text{A.5})$$

Thus, the proof is complete.

APPENDIX B: PROOF OF LEMMA 3

In order to obtain the coverage probability of the typical user in the near user case, and based on SINR analysis in (6) and (10), we can have

$$|h_t|^2 < M_{t*} (\sigma^2 + I_\Psi) r_t^\alpha. \quad (\text{B.1})$$

Then, we derive the conditional coverage probability of the typical user as

$$\begin{aligned} P_{cov,t}(r) &= \mathbb{E}_{I_\Psi} \{ P(|h_w|^2 < M_{t*} (\sigma^2 + I_\Psi) r_t^\alpha) \} \\ &= \exp(-mM_{t*}\sigma^2 r_t^\alpha) \mathbb{E}_{I_\Psi} \{ \exp(-mM_{t*}I_\Psi r_t^\alpha) \} \sum_{n=0}^{m-1} \frac{(mM_{t*}(\sigma^2 + I_\Psi) r_t^\alpha)^n}{n!} \\ &= \sum_{n=0}^{m-1} \sum_{p=0}^n \binom{n}{p} \frac{r_t^{\alpha n} (-1)^n}{n!} \underbrace{\exp(-mM_{t*}\sigma^2 r_t^\alpha) (-mM_{t*}\sigma^2)^p}_{\Lambda_1} \underbrace{\mathbb{E}_{I_\Psi} \{ \exp(-mM_{t*}I_\Psi r_t^\alpha) \} (-mM_{t*}I_\Psi)^{n-p}}_{\Lambda_2}. \end{aligned} \quad (\text{B.2})$$

Using the fact that

$$\left. \frac{d^p (\exp(-mM_{t*}\sigma^2 y))}{dy^p} \right|_{y=r_t^\alpha} = \exp(-mM_{t*}\sigma^2 r_t^\alpha) (-mM_{t*}\sigma^2)^p, \quad (\text{B.3})$$

we can have

$$\Lambda_1 = \left. \frac{d^p (\exp(-mM_{t*}\sigma^2 y))}{dy^p} \right|_{y=r_t^\alpha}. \quad (\text{B.4})$$

Now, we apply the Fa à di Bruno's formula to solve the derivative of p -th order as follows:

$$\Lambda_1 = \exp(-mM_{t*}\sigma^2 r_t^\alpha) \sum_{j=1}^p p! \prod_{j=1}^p \frac{\left((-mM_{t*}\sigma^2) \prod_{k=0}^{j-1} (1-k) r_t^{\alpha(1-j)} \right)^{q_j}}{q_j! (j!)^{q_j}}, \quad (\text{B.5})$$

where the sum q_j is over all p -tuples of nonnegative integers satisfying the constraint

$$1 \cdot q_1 + 2 \cdot q_2 + \cdots + p \cdot q_p = p. \quad (\text{B.6})$$

Similar to the steps from (B.3) to (B.5), Λ_2 can be expressed to

$$\begin{aligned}\Lambda_2 &= \mathbb{E}_{I_\Psi} \left\{ \exp(-m M_{t*} I_\Psi r_t^\alpha) (-m M_{t*} I_\Psi)^{n-p} \right\} \\ &= \mathbb{E}_{I_\Psi} \left\{ \frac{d^{n-p} (\exp(-m M_{t*} I_\Psi y))}{dy^{n-p}} \bigg|_{y=r_t^\alpha} \right\} \\ &= \frac{d^{n-p} (m \mathcal{L}_t(M_{t*} y))}{dy^{n-p}} \bigg|_{y=r_t^\alpha}.\end{aligned}\tag{B.7}$$

It's challenging to derive $(n-p)$ -th order derivation of incomplete Beta function directly. Thus, the derived incomplete Beta function in (12) can be written to

$$\begin{aligned}B\left(\frac{-sP_U}{m_I r_t^\alpha}; i-\delta, 1-m_I\right) &= \left(\frac{-sP_U}{m_I r_t^\alpha}\right)^{(i-\delta)} \frac{1}{i-\delta} {}_2F_1\left(1-\delta, m_I; 2-\delta; \left(\frac{-sP_U}{m_I r_t^\alpha}\right)\right) \\ &= \left(\frac{-sP_U}{m_I r_t^\alpha}\right)^{(i-\delta+a)} \sum_{a=0}^{\infty} \frac{(m_I)_a}{a! (i-\delta+a)},\end{aligned}\tag{B.8}$$

where $(m_I)_a$ denotes a Pochhammer symbol, which can be calculated as $\frac{\Gamma(m_I+a)}{\Gamma(m_I)}$.

Thus, the Laplace transform can be rewritten to

$$\mathcal{L}_t(s) = \exp\left(-\frac{2\pi\lambda}{\alpha} \sum_{a=0}^{\infty} \frac{(m_I)_a}{a! (i-\delta+a)} \sum_{i=1}^{m_I} \binom{m_I}{i} \left(\frac{sP_U}{m_I}\right)^{i+a} (-1)^a r_t^{-\alpha(i-\delta+a)}\right).\tag{B.9}$$

Then, substituting (B.9) into (B.7), and using Fa à di Bruno's formula, (B.7) can be transformed into

$$\begin{aligned}\Lambda_2 &= \frac{d^{n-p} (\exp(-\Lambda_3 y^\delta))}{dy^{n-p}} \bigg|_{y=r_t^\alpha} \\ &= \exp(-\Lambda_3 r_t^2) \sum (n-p)! \prod_{b=1}^{n-p} \frac{\left((- \Lambda_3) \prod_{k=0}^{b-1} (\delta-k) r_t^{2-\alpha b}\right)^{q_b}}{q_b! (b!)^{q_b}},\end{aligned}\tag{B.10}$$

where $\Lambda_3 = \frac{2\pi\lambda}{\alpha} \sum_{a=0}^{\infty} \frac{(m_I)_a}{a! (i-\delta+a)} \sum_{i=1}^{m_I} \binom{m_I}{i} \left(\frac{M_{t*} P_U}{m_I}\right)^{i+a} (-1)^a$, and q_b is over all $(n-p)$ -tuples of nonnegative integers satisfying the constraint $1 \cdot q_1 + 2 \cdot q_2 + \dots + (n-p) \cdot q_b = (n-p)$.

Substituting (B.5) and (B.10) into (B.2), we can derive the conditional coverage probability for the typical user in the near user case, as given in (14). The proof is complete.

APPENDIX C: PROOF OF LEMMA 5

Unlike the User-Centric strategy, the first interfering UAV is necessary to evaluate separately in the UAV-Centric strategy. In this section, we evaluate the Laplace transform of inter-cell

interference of the near user in the UAV-Centric strategy, where the inter-cell interference experience at the near user can be given by

$$I_{w,\Psi} = \underbrace{\sum_{j \in \Psi, d_j > D} |g_j|^2 P_U d_j^{-\alpha}}_{I_2} + \underbrace{|g_1|^2 P_U D^{-\alpha}}_{I_1}, \quad (\text{C.1})$$

where I_1 denotes the received power from the interfering UAV at the distance D , and I_2 denotes the received power from all other interfering UAVs except the one located at the distance D . For the near user at the typical cell, the Laplace transform of interference power distribution conditioned on the serving distance D is given by

$$\begin{aligned} \mathcal{L}_w(s|D) &= \mathbb{E} \left\{ \exp(-s I_{w,\Psi}) | D \right\} = \mathbb{E} \left\{ \exp \left(-s \sum_{j \in \Psi, d_j > D} |g_j|^2 \frac{P_U}{m_I} d_j^{-\alpha} - s |g_1|^2 \frac{P_U}{m_I} D^{-\alpha} \right) \middle| D \right\} \\ &= \mathbb{E}_d \left\{ \exp \left(-s \sum_{j \in \Psi} \mathbb{E}_g \{ |g_j|^2 \} \frac{P_U}{m_I} d_j^{-\alpha} - s \mathbb{E}_g \{ |g_1|^2 \} \frac{P_U}{m_I} D^{-\alpha} \right) \middle| D \right\}. \end{aligned} \quad (\text{C.2})$$

We first evaluate the Laplace transform of I_2 . Using the MGF of Gamma random variable $|g_j|$, and after some algebraic manipulations, I_2 can be rewritten to

$$I_2 = \exp \left(-2\pi\lambda_U \int_{l_I}^{\infty} \left(1 - \mathbb{E}_g \left\{ \exp \left(-s |g_j|^2 \frac{P_U}{m_I} r^{-\alpha} \right) \right\} \right) r dr \right), \quad (\text{C.3})$$

where $l_I = \sqrt{D^2 + h^2}$.

Similar to the arguments from (A.2) to (A.5), the Laplace transform of I_2 can be obtained as

$$I_2 = \exp \left(-\frac{2\pi\lambda_U}{\alpha} \sum_{i=1}^{m_I} \binom{m_I}{i} \left(\frac{s P_U}{m_I} \right)^{\delta} (-1)^{(\delta-i)} B \left(\frac{-s P_U}{l_I^{\alpha} m_I}; i - \delta, 1 - m_I \right) \right). \quad (\text{C.4})$$

Note that the MGF derived in (C.4) does not include the interfering UAV at the distance D strictly, which is actually the largest interference source. Therefore, using Poisson Hole Process (PHP), the first interference located at distance D can be derived as follows:

$$I_1 = \exp \left(\frac{-2\pi}{\pi(D + \varepsilon)^2 - \pi(D - \varepsilon)^2} \int_{l_I - \varepsilon}^{l_I + \varepsilon} \left(1 - \mathbb{E}_g \left\{ \exp \left(-s |g_1|^2 \frac{P_U}{m_I} l_I^{-\alpha} \right) \right\} \right) r dr \right), \quad (\text{C.5})$$

where ε is a small distance to evaluate the first interference UAV.

With the aid of Laplace transform for the Nakagami- m distribution with fading parameter m_I ,

we can obtain $\mathbb{E}_g \left\{ |g_1|^2 \frac{P_U}{m_I} d_1^{-\alpha} \right\} = \left(1 + \frac{sP_U l_I^{-\alpha}}{m_I} \right)^{-m_I}$. As such, the Laplace transform of the first interfering UAV can be rewritten to

$$\begin{aligned} I_1 &= \exp \left(\frac{-1}{2D\varepsilon} \int_{l_I-\varepsilon}^{l_I+\varepsilon} \left(1 - \left(1 + \frac{sP_U}{m_I l_I^\alpha} \right)^{-m_I} \right) r dr \right) \\ &= \exp \left(-\frac{l_I}{D} + \frac{l_I}{D} \left(1 + \frac{sP_U}{l_I^\alpha m_I} \right)^{-m_I} \right). \end{aligned} \quad (\text{C.6})$$

Based on (C.4) and (C.6), we can obtain the Laplace transform of the near user for the UAV-Centric strategy as given in (23). The proof is complete.

APPENDIX D: PROOF OF LEMMA 6

In order to prove the desired result, and according to Newton's Generalization of the binomial theorem [34], we first transform (C.6) into

$$I_1 = \exp \left(-\frac{l_I}{D} + \frac{l_I}{D} \sum_{u=0}^{\infty} (-1)^u C_{m_I+u+1}^{ru} \left(\frac{sP_U}{l_I^\alpha m_I} \right)^u \right), \quad (\text{D.1})$$

where $C_{m_I+u+1}^u = \frac{(m_I+u+1)(m_I+u)\cdots(m_I+2)}{k!}$.

According to the SINR expressions of (19) and (20), and similar to Appendix B, we can derive the conditional coverage probability on the serving distance D of the near user in the UAV-Centric strategy to

$$P_{cov,w}(r|D) = \exp(-mM_{w*}(\sigma^2 + I_1 + I_2)r_w^\alpha) \sum_{n=0}^{m-1} \frac{(mM_{w*}(\sigma^2 + I_1 + I_2)r_w^\alpha)^n}{n!}. \quad (\text{D.2})$$

By applying polynomial expansion to (D.2), the coverage probability can be rewritten to

$$\begin{aligned} P_{cov,w}(r|D) &= \sum_{n=0}^{m-1} \sum_{k=0}^n \sum_{l=0}^k \frac{(-1)^n r_w^{\alpha n}}{l!(k-l)!(n-k)!} \exp(-mM_{w*}\sigma^2 r_w^\alpha) (-mM_{w*}\sigma^2)^{n-k} \\ &\quad \times \mathbb{E}_{I_1} \left\{ \exp(-mM_{w*}I_1 r_w^\alpha) (-mM_{w*}I_1)^{k-l} \right\} \mathbb{E}_{I_2} \left\{ \exp(-mM_{w*}I_2 r_w^\alpha) (-mM_{w*}I_2)^l \right\}. \end{aligned} \quad (\text{D.3})$$

Following the similar steps from (B.2) to (B.10), and according to Fa à di Bruno's formula,

we can readily derive that the first interference I_1 to

$$\left. \frac{d^{k-l} \mathcal{L}(M_{w*} x)}{dx^{k-l}} \right|_{x=r_w^\alpha} = \exp \left(-\frac{l_I m}{D} + \Theta_2 r_w^{\alpha u} \right) \sum (k-l)! \prod_{j=1}^{k-l} \frac{\left((-\Theta_2) \prod_{p=0}^{j-1} (u-p) r_w^{\alpha(u-j)} \right)^{q_u}}{q_u! (j!)^{q_u}}, \quad (\text{D.4})$$

where $\Theta_2 = \frac{l_I m}{D} \sum_{u=0}^{\infty} (-1)^u C_{m_I+u+1}^u \left(\frac{M_{w*} P_I}{l_I^\alpha m_I} \right)^u$. Then, the closed-form expression of the coverage probability for the near user in (25) can be obtained. Thus, the Lemma is proved.

APPENDIX E: PROOF OF THEOREM 2

In this appendix, we focus on drive the coverage probability of the near user. Using the PDF of (21), the coverage probability of the near user conditioned on the serving distance can be obtained by

$$P_{cov,w}(D) = \int_0^{l_1} P_{cov,w}(r) f_{R|D}(r|D) dr \quad (\text{E.1})$$

The overall coverage probability can be derived by the serving distance of multi-UAV networks, which can be expressed as

$$P_{cov,w} = \int_0^{\infty} P_{cov,w}(D) f_D(D) dD. \quad (\text{E.2})$$

Plugging (11) into (E.2), and after some mathematical manipulations, the coverage probability of the near user can be obtained. Thus, the proof is complete.

REFERENCES

- [1] T. Hou, Y. Liu, Z. Song, X. Sun, and Y. Chen, "Non-orthogonal multiple access in multi-UAV networks," in *Int. Proc. Commun. Conf. (ICC)*, Shanghai, China, May 2019, pp. 1–1.
- [2] Y. Zeng, R. Zhang, and T. J. Lim, "Wireless communications with unmanned aerial vehicles: opportunities and challenges," *IEEE Commun. Mag.*, vol. 54, no. 5, pp. 36–42, May 2016.
- [3] M. Mozaffari, W. Saad, M. Bennis, and M. Debbah, "Unmanned aerial vehicle with underlaid device-to-device communications: Performance and tradeoffs," *IEEE Trans. Wireless Commun.*, vol. 15, no. 6, pp. 3949–3963, Jun. 2016.
- [4] A. A. Khuwaja, Y. Chen, N. Zhao, M. Alouini, and P. Dobbins, "A survey of channel modeling for UAV communications," *IEEE Commun. Surveys Tuts.*, pp. 1–1, 2018.
- [5] A. Goldsmith, *Wireless Communication*. Cambridge University Press, 2nd ed, 2010.
- [6] Z. Ding, Y. Liu, J. Choi, Q. Sun, M. Elkashlan, C. I, and H. V. Poor, "Application of non-orthogonal multiple access in LTE and 5G networks," *IEEE Commun. Magazine*, vol. 55, no. 2, pp. 185–191, Feb. 2017.
- [7] Z. Qin, J. Fan, Y. Liu, Y. Gao, and G. Y. Li, "Sparse representation for wireless communications: A compressive sensing approach," *IEEE Signal Process. Mag.*, vol. 35, no. 3, pp. 40–58, May 2018.

- [8] Z. Ding, P. Fan, and H. V. Poor, "Impact of user pairing on 5G nonorthogonal multiple-access downlink transmissions," *IEEE Trans. Veh. Technol.*, vol. 65, no. 8, pp. 6010–6023, Aug. 2016.
- [9] Y. Liu, Z. Qin, M. ElKashlan, Z. Ding, A. Nallanathan, and L. Hanzo, "Nonorthogonal multiple access for 5G and beyond," *Proc. of the IEEE*, vol. 105, no. 12, pp. 2347–2381, Dec. 2017.
- [10] S. M. R. Islam, M. Zeng, O. A. Dobre, and K. Kwak, "Resource allocation for downlink NOMA systems: Key techniques and open issues," *IEEE Wireless Commun.*, vol. 25, no. 2, pp. 40–47, Apr. 2018.
- [11] S. M. R. Islam, N. Avazov, O. A. Dobre, and K. Kwak, "Power-domain non-orthogonal multiple access (NOMA) in 5G systems: Potentials and challenges," *IEEE Commun. Surveys Tuts.*, vol. 19, no. 2, pp. 721–742, Secondquarter 2017.
- [12] Z. Qin, X. Yue, Y. Liu, Z. Ding, and A. Nallanathan, "User association and resource allocation in unified non-orthogonal multiple access enabled heterogeneous ultra dense networks," *IEEE Commun. Mag.*, vol. 56, no. 6, pp. 86–92, Jun. 2018.
- [13] N. Goddemeier and C. Wietfeld, "Investigation of air-to-air channel characteristics and a UAV specific extension to the Rice model," in *2015 IEEE Globecom Workshops (GC Wkshps)*, Dec. 2015, pp. 1–5.
- [14] F. Jiang and A. L. Swindlehurst, "Optimization of UAV heading for the ground-to-air uplink," *IEEE J. Sel. Areas Commun.*, vol. 30, no. 5, pp. 993–1005, Jun. 2012.
- [15] M. Mozaffari, W. Saad, M. Bennis, and M. Debbah, "Efficient deployment of multiple unmanned aerial vehicles for optimal wireless coverage," *IEEE Commun. Lett.*, vol. 20, no. 8, pp. 1647–1650, Aug. 2016.
- [16] V. V. Chetlur and H. S. Dhillon, "Downlink coverage analysis for a finite 3-D wireless network of unmanned aerial vehicles," *IEEE Trans. Commun.*, vol. 65, no. 10, pp. 4543–4558, Oct. 2017.
- [17] S. Zhang, Y. Zeng, and R. Zhang, "Cellular-enabled UAV communication: A connectivity-constrained trajectory optimization perspective," *arXiv*, vol. 1805.07182v1, pp. 1–1, May 2018.
- [18] L. Liu, S. Zhang, and R. Zhang, "Exploiting NOMA for multi-beam UAV communication in cellular uplink," *arXiv*, vol. 1810.10839v1, pp. 1–1, Oct. 2018.
- [19] Z. Ding, Z. Yang, P. Fan, and H. V. Poor, "On the performance of non-orthogonal multiple access in 5G systems with randomly deployed users," *IEEE Signal Process. Lett.*, vol. 21, no. 12, pp. 1501–1505, Dec. 2014.
- [20] Y. Liu, Z. Ding, M. ElKashlan, and H. V. Poor, "Cooperative non-orthogonal multiple access with simultaneous wireless information and power transfer," *IEEE J. Sel. Areas Commun.*, vol. 34, no. 4, pp. 938–953, Apr. 2016.
- [21] X. Yue, Y. Liu, S. Kang, A. Nallanathan, and Y. Chen, "Modeling and analysis of two-way relay non-orthogonal multiple access systems," *IEEE Trans. Commun.*, vol. 66, no. 9, pp. 3784–3796, Sep. 2018.
- [22] T. Hou, X. Sun, and Z. Song, "Outage performance for non-orthogonal multiple access with fixed power allocation over Nakagami- m fading channels," *IEEE Commun. Lett.*, vol. 22, no. 4, pp. 744–747, Apr. 2018.
- [23] Y. Mao, B. Clerckx, and V. O. K. Li, "Rate-splitting for downlink multi-user multi-antenna systems: Bridging NOMA and conventional linear precoding," *arXiv*, vol. 1710.11018v1, pp. 1–1, Aug. 2017.
- [24] —, "Rate-splitting for multi-antenna non-orthogonal unicast and multicast transmission: Spectral and energy efficiency analysis," *arXiv*, vol. 1808.08325v1, pp. 1–1, Aug. 2018.
- [25] Y. Liu, Z. Qin, M. ElKashlan, Y. Gao, and L. Hanzo, "Enhancing the physical layer security of non-orthogonal multiple access in large-scale networks," *IEEE Trans. Wireless Commun.*, vol. 16, no. 3, pp. 1656–1672, Mar. 2017.
- [26] T. Qi, W. Feng, and Y. Wang, "Outage performance of non-orthogonal multiple access based unmanned aerial vehicles satellite networks," *China Communications*, vol. 15, no. 5, pp. 1–8, May 2018.
- [27] T. Hou, Y. Liu, Z. Song, X. Sun, and Y. Chen, "Multiple antenna aided NOMA in UAV networks: A stochastic geometry approach," *IEEE Trans. Commun.*, pp. 1–14, 2018 Accept to appear.
- [28] Y. Liu, Z. Qin, Y. Cai, Y. Gao, G. Y. Li, and A. Nallanathan, "UAV communications based on non-orthogonal multiple access," *arXiv*, vol. 1809.05767v1, pp. 1–1, Sep. 2018.

- [29] X. Liu, Y. Liu, Y. Chen, and L. Hanzo, "Trajectory design and power control for multi-UAV assisted wireless networks: A machine learning approach," *arXiv*, vol. 1812.07665v1, pp. 1–1, Dec. 2018.
- [30] T. M. Nguyen, W. Ajib, and C. Assi, "A novel cooperative NOMA for designing UAV-assisted wireless backhaul networks," *IEEE J. Sel. Areas Commun.*, vol. 36, no. 11, pp. 2497–2507, Nov. 2018.
- [31] W. Mei and R. Zhang, "Uplink cooperative NOMA for cellular-connected UAV," *arXiv*, vol. 1809.03657v2, pp. 1–1, Sep. 2018.
- [32] K. Han, K. Huang, and R. W. Heath, "Connectivity and blockage effects in millimeter-wave air-to-everything networks," *IEEE Wireless Commun. Lett.*, pp. 1–1, 2018.
- [33] I. S. Gradshteyn and I. M. Ryzhik, *Table of Integrals, Series and Products*. New York: Academic Press, 6th ed, 2000.
- [34] N. Bourbaki, *Elements of the History of Mathematics Paperback*. Springer Berlin Heidelberg, 2nd ed, 2008.